

# Iterative Prewhitening for Multidimensional Harmonic Retrieval: New Variants and Comparative Study

Kefei Liu<sup>1</sup>, João Paulo C. L. da Costa<sup>2</sup>, H. C. So<sup>1</sup>, and Rafael Timóteo de Sousa Júnior<sup>2</sup>

<sup>1</sup>Department of Electronic Engineering, City University of Hong Kong, Kowloon, Hong Kong

<sup>2</sup>Department of Electrical Engineering, University of Brasília, Brasília, Brazil

Email: kefeiliu@ieee.org, jpdacosta@unb.br, hcso@ee.cityu.edu.hk, desousa@unb.br

**Abstract**—In the presence of colored noise, subspace based harmonic retrieval algorithms suffer a performance degradation due to the interference between signal and noise subspaces. In order to efficiently separate the signal and noise subspaces, prewhitening is applied to decorrelate the noise samples prior to harmonic retrieval. When noise-only observations are unavailable for estimating the noise statistics, recently we have proposed an iterative algorithm for joint multidimensional prewhitening and harmonic retrieval. In this algorithm, harmonic retrieval can be applied during the iterations or only after convergence, and there are two ways to initialize the prewhitening matrices, leading to four variants. In this work, we investigate and compare these variants of the iterative prewhitening algorithms. Our study shows that, ignoring the parametric signal structure during the iterations leads to more stable performance with higher probability of global convergence. In spite of this, under medium-to-high signal-to-noise ratio conditions, the iterative prewhitening algorithm without exploiting the parametric signal structure may converge more slowly than that does.

**Keywords**—Prewhitening, Kronecker colored noise, harmonic retrieval, tensor ESPRIT, multilinear algebra.

## I. INTRODUCTION

Retrieval of harmonics from  $R$ -dimensional ( $R$ -D) noisy measurements, where  $R \geq 2$ , has a variety of applications ranging from radar to mobile communications and medical imaging. Subspace approaches to  $R$ -D harmonic retrieval (HR) such as  $R$ -D ESPRIT [1], [2],  $R$ -D MUSIC [3], and PUMA [4] utilize the signal and noise subspaces for HR. In the presence of colored noise, due to noise correlation, most of the noise energy is contained in a small fraction of the whole space spanned by a few principal eigenvectors. This may interfere the estimation of the signal subspace and leads to a performance degradation of the parameter estimation. Prewhitening decorrelates the noise components, so that the noise power is uniformly distributed over the whole noise subspace, which facilitates the separation of the signal and noise subspaces and hence improves the estimation performance.

In [5], multidimensional prewhitening algorithms have been proposed in order to improve the performance of multidimensional parameter estimators. By exploiting the Kronecker structure of the noise correlation matrix, accurate noise modeling can be achieved with a few noise-only measurements for estimation of the noise statistics, leading to good separation of the signal and noise subspaces and noise reduction and hence an improved accuracy of subsequent HR. When noise-only

observations are unavailable for estimating the noise statistics, an iterative algorithm for joint multidimensional prewhitening and HR is employed. In this algorithm, HR can be incorporated in each iteration or only applied after convergence, and there are two ways to initialize the prewhitening matrices, leading to four variants. In this work, we investigate and compare these variants of the iterative multidimensional prewhitening (I-MD-PWT) algorithms under different signal-to-noise ratio (SNR) conditions. Our study shows that, ignoring the parametric signal structure during the iterations leads to more stable performance as well as higher probability of global convergence. Still, for medium-to-high SNRs the iterative prewhitening algorithm without exploiting the parametric signal structure may converge more slowly than that does.

## II. DATA MODEL

*Notation:* The superscripts  $\text{T}$ ,  $\text{H}$ , and  $\dagger$  stand for transposition, Hermitian transposition, and Moore-Penrose pseudo inverse, respectively. The  $r$ -mode vectors of a tensor  $\mathcal{T} \in \mathbb{C}^{I_1 \times \dots \times I_R}$  are obtained by varying the  $r$ -th index within its range  $(1, \dots, I_r)$  and keeping all the other indices fixed. The  $r$ -mode unfolding of  $\mathcal{T}$ , symbolized by  $[\mathcal{T}]_{(r)} \in \mathbb{C}^{I_r \times (I_1 \dots I_{r-1} I_{r+1} \dots I_R)}$ , represents the matrix consisting of its  $r$ -mode vectors. The  $r$ -mode product of  $\mathcal{T}$  and a matrix  $U \in \mathbb{C}^{J_r \times I_r}$  along the  $r$ -th mode is denoted as  $\mathcal{T} \times_r U \in \mathbb{C}^{I_1 \times \dots \times J_r \times \dots \times I_R}$ . It is obtained by multiplying the  $r$ -mode vectors of  $\mathcal{T}$  from the left-hand side by  $U$  [6].

Consider the uniform multidimensional HR problem [7], where the noisy observations are modeled as a superposition of  $d$   $R$ -D complex sinusoids (cisoids) and colored noise with a Kronecker correlation structure [8]–[10]:

$$\mathcal{X} = \sum_{i=1}^d \mathbf{a}_i^{(1)} \circ \dots \circ \mathbf{a}_i^{(R)} \circ \mathbf{s}_i^{\text{T}} + \mathcal{N}^{(c)}, \quad (1)$$

where  $\mathbf{a}_i^{(r)} = [1, e^{j\mu_i^{(r)}}, \dots, e^{j(M_r-1)\mu_i^{(r)}}]^{\text{T}} \in \mathbb{C}^{M_r \times 1}$  is the steering vector associated with the  $i$ -th source in the  $r$ -th mode,  $i = 1, \dots, d$ ,  $r = 1, \dots, R$ , with  $\{\mu_i^{(r)}\}$  being the spatial frequencies, and  $\mathbf{s}_i \in \mathbb{C}^{1 \times M_{R+1}}$  contains the samples of the  $i$ -th signal with  $M_{R+1} = N$ , standing for the number of snapshots.

The  $\mathcal{N}^{(c)} \in \mathbb{C}^{M_1 \times \dots \times M_R \times N}$  collects Kronecker colored noise samples which are characteristic by the following correlation structure:

$$\mathbf{C} = \mathbf{C}_{R+1} \otimes \dots \otimes \mathbf{C}_1, \quad (2)$$

where  $\mathbf{C} \in \mathbb{C}^{(M_1 \dots M_R N) \times (M_1 \dots M_R N)}$  and  $\mathbf{C}_r \in \mathbb{C}^{M_r \times M_r}$ ,  $r = 1, \dots, R+1$ , respectively, denote the noise covariance matrix in all modes and  $r$ -th mode [5]. The multidimensional Kronecker colored noise exists in EEG/MEG [10] and MIMO [9] applications. The  $\mathcal{N}^{(c)}$  can be expressed as

$$\mathcal{N}^{(c)} = \mathcal{N} \times_1 \mathbf{L}_1 \cdots \times_{R+1} \mathbf{L}_{R+1}, \quad (3)$$

where  $\mathcal{N} \in \mathbb{C}^{M_1 \times \dots \times M_R \times N}$  is a tensor collecting i.i.d. zero-mean circularly symmetric complex Gaussian (ZMCSCG) noise samples of variance  $\sigma_n^2$  [5], and  $\mathbf{L}_r \in \mathbb{C}^{M_r \times M_r}$ ,  $r = 1, \dots, R+1$ , is the correlation factor in the  $r$ -th mode satisfying  $\mathbf{C}_r = \mathbf{L}_r \cdot \mathbf{L}_r^H$ .

Defining  $\mathbf{A}^{(r)} = [\mathbf{a}_1^{(r)}, \dots, \mathbf{a}_d^{(r)}] \in \mathbb{C}^{M_r \times d}$ ,  $r = 1, \dots, R$ , and letting  $\mathbf{S}^T = \mathbf{A}^{(R+1)} = [\mathbf{s}_1, \dots, \mathbf{s}_d] \in \mathbb{C}^{N \times d}$  which collects the source samples over all  $N$  snapshots, (1) can be rewritten in terms of  $r$ -mode products as

$$\mathcal{X} = \mathcal{I}_{R+1,d} \times_1 \mathbf{A}^{(1)} \cdots \times_R \mathbf{A}^{(R)} \times_{R+1} \mathbf{S}^T + \mathcal{N}^{(c)}, \quad (4)$$

where  $\mathcal{I}_{R+1,d}$  represents the  $R$ -D identity tensor of size  $d \times \dots \times d$ , whose elements are equal to one when the indices  $i_1 = \dots = i_{R+1}$  and zero otherwise.

Letting

$$\mathcal{A} = \mathcal{I}_{R+1,d} \times_1 \mathbf{A}^{(1)} \cdots \times_R \mathbf{A}^{(R)}, \quad (5)$$

(4) can be expressed in a more compact form as

$$\mathcal{X} = \mathcal{A} \times_{R+1} \mathbf{S}^T + \mathcal{N}^{(c)}. \quad (6)$$

The SNR is

$$\text{SNR} = \frac{\|\mathcal{A} \times_{R+1} \mathbf{S}^T\|_F^2}{M_1 \dots M_R N \sigma_n^2}, \quad (7)$$

where  $\|\cdot\|_F$  represents the Frobenius norm of a matrix or tensor, which is defined as the square root of the sum of the squared amplitudes of its elements. Given  $\mathcal{X}$  and the number of components  $d$ , the objective is to estimate  $\mu_i^{(r)}$ ,  $r = 1, \dots, R$ ,  $i = 1, \dots, d$ .

### III. ITERATIVE MULTIDIMENSIONAL PREWHITENING WITHOUT NOISE SAMPLES

The prewhitening process typically requires the independent (secondary) noise-only observations to estimate the noise statistics. In case noise-only observations are unavailable, an iterative algorithm for joint prewhitening and HR has been proposed in [5]. In this section, its four variants are presented.

#### A. Iterative Prewhitening and Signal Estimation

In the first scheme, denoted as I-MD-PWT I, the parametric structure of the signals is ignored during the iterations. The iterative algorithm for joint noise estimation, prewhitening and signal estimation is described in Table I.

The variation of the estimated noise tensor  $\hat{\mathcal{N}}^{(c)}$  (i.e., signal reconstruction error) can be used as a measure to terminate the iterations. In [5], an adaptive threshold that varies with the noise power is employed in the termination criterion such that the iterations stop at an optimal number of iterations.

Table I. ITERATIVE ALGORITHM FOR JOINT NOISE ESTIMATION, PREWHITENING AND SIGNAL ESTIMATION

*Initialization:* The prewhitening matrices (correlation factors) are set as identity matrices:  $\hat{\mathbf{L}}_r = \mathbf{I}_{M_r}$ ,  $r = 1, \dots, R+1$ ;

- (1) Higher-order SVD (HOSVD) based low-rank approximation of  $\mathcal{X}$  [6]:

$$\check{\mathcal{X}} = \mathcal{S}^{[t]} \times_1 \mathbf{U}_1^{[t]} \cdots \times_{R+1} \mathbf{U}_{R+1}^{[t]} \in \mathbb{C}^{M_1 \times \dots \times M_{R+1}}, \quad (8)$$

where  $\mathcal{S}^{[t]} \in \mathbb{C}^{p_1 \times \dots \times p_{R+1}}$ , and  $\mathbf{U}_r^{[t]} \in \mathbb{C}^{M_r \times p_r}$  with  $p_r = \min(M_r, d)$ ,  $r = 1, \dots, R+1$ , are truncated to the  $d$  columns corresponding to the  $d$  largest singular values.

- (2) Noise estimation:

$$\hat{\mathcal{N}}^{(c)} = \mathcal{X} - \check{\mathcal{X}}.$$

- (3) Estimation of correlation factors  $\hat{\mathbf{L}}_r$ ,  $r = 1, \dots, R+1$ .

- (3.1) Estimation of  $\mathbf{C}_r$ ,  $r = 1, \dots, R+1$

$$\hat{\mathbf{C}}_r = \frac{1}{\beta_r} \left[ \hat{\mathcal{N}}^{(c)} \right]_{(r)} \left[ \hat{\mathcal{N}}^{(c)} \right]_{(r)}^H.$$

where  $\beta_r$  is the normalization coefficient such that  $\text{tr}(\hat{\mathbf{C}}_r) = M_r$ .

- (3.2) Cholesky decomposition:

$$\hat{\mathbf{C}}_r = \hat{\mathbf{L}}_r \hat{\mathbf{L}}_r^H, \quad r = 1, \dots, R+1.$$

- (4) Prewhitening and dewhitening.

- (4.1) Prewhitening:

$$\mathcal{X}' = \mathcal{X} \times_1 \hat{\mathbf{L}}_1^{-1} \cdots \times_{R+1} \hat{\mathbf{L}}_{R+1}^{-1}. \quad (9)$$

- (4.2) HOSVD based low-rank approximation of  $\mathcal{X}'$ :

$$\check{\mathcal{X}}' = \mathcal{S}^{[t]} \times_1 \mathbf{U}_1^{[t]} \cdots \times_{R+1} \mathbf{U}_{R+1}^{[t]}. \quad (10)$$

- (4.3) Dewhitening:

$$\begin{aligned} \check{\mathcal{X}} &= \check{\mathcal{X}}' \times_1 \hat{\mathbf{L}}_1 \cdots \times_{R+1} \hat{\mathbf{L}}_{R+1} \\ &= \mathcal{S}^{[t]} \times_1 \left( \hat{\mathbf{L}}_1 \mathbf{U}_1^{[t]} \right) \cdots \\ &\quad \times_{R+1} \left( \hat{\mathbf{L}}_{R+1} \mathbf{U}_{R+1}^{[t]} \right). \end{aligned}$$

- (5) Repeat Steps (2)-(4) until convergence or the maximum number of iterations is reached.

Note that compared with [5], here the signal parameter step has been removed. It has been shown through extensive simulations that for low-to-intermediate SNRs the simplified prewhitening scheme leads to smaller estimation error with a higher probability of convergence than the original version, while for high SNRs, with slightly more iterations it also converges to a state with the same estimation error as the original one.

After convergence, the frequencies  $\{\mu_i^{(r)}\}$  are extracted by applying the unitary tensor-ESPRIT (UTE) [2] on the following signal subspace tensor

$$\check{\mathcal{U}}^{[s]} = \mathcal{S}^{[t]} \times_1 \left( \hat{\mathbf{L}}_1 \cdot \mathbf{U}_1^{[t]} \right) \cdots \times_R \left( \hat{\mathbf{L}}_R \cdot \mathbf{U}_R^{[t]} \right).$$

#### B. Iterative Prewhitening and Harmonic Retrieval

In the second scheme, denoted as I-MD-PWT II, the parametric structure of signals is exploited during the iterations. That is, additional HR steps shown below are incorporated in

Step (2) of the algorithm in Table I. As shown in Section IV, such a scheme of exploiting the parametric signal structure enjoys faster convergence under high SNR conditions.

- 
- (2.1) The estimates of the spatial frequencies at the  $k$ -th iteration, denoted as  $\hat{\mu}_{k,i}^{(r)}$ ,  $r = 1, \dots, R$ ,  $i = 1, \dots, d$ , are obtained by applying the UTE on the signal subspace tensor  $\tilde{\mathcal{U}}^{[s]}$ , or by applying the closed-form PARAllel FACTor decomposition [11] based parameter estimator (CFP-PE) on  $\tilde{\mathcal{X}}$ .
- (2.2) From  $\hat{\mu}_{k,i}^{(r)}$ ,  $r = 1, \dots, R$ ,  $i = 1, \dots, d$ , compute  $\hat{\mathcal{A}}_k$  according to (5). Using  $\mathcal{X}$  and  $\hat{\mathcal{A}}_k$ , calculate  $\hat{\mathcal{S}}_k = \left( [\mathcal{X}]_{(R+1)} \cdot [\hat{\mathcal{A}}_k]_{(R+1)}^\dagger \right)^\top$ .
- (2.3) The noise tensor  $\hat{\mathcal{N}}_k^{(c)}$  is estimated as  $\hat{\mathcal{N}}_k^{(c)} = \mathcal{X} - \hat{\mathcal{A}}_k \times_{R+1} \hat{\mathcal{S}}_k^\top$ .
- 

In I-MD-PWT I and I-MD-PWT II, the prewhitening matrices  $\mathbf{L}_r$ ,  $r = 1, \dots, R+1$ , are initialized as identity matrices. Under low SNR conditions where the noise components of the signal-plus-noise measurements  $\mathcal{X}$  are much stronger than the signal components,  $\mathcal{X}$  itself can be considered as an approximation of  $\mathcal{N}^{(c)}$ . Therefore, alternatively,  $\mathbf{L}_r$ ,  $r = 1, \dots, R+1$ , can be initialized from  $\mathcal{X}$ . Note that in this case, additional prewhitening and dewhitening steps are required in Step (1) of the iterative algorithm described in Table I. As a result, we have four variants for the I-MD-PWT algorithm, as shown in Table II.

Table II. VARIANTS OF I-MD-PWT SCHEMES.

	Initial guess of $\hat{\mathbf{L}}_r$	Harmonic retrieval
I-MD-PWT I	$\mathbf{I}_{M_r}$	after convergence
I-MD-PWT II	$\mathbf{I}_{M_r}$	each iteration
I-MD-PWT III	estimated from $\hat{\mathcal{N}}^{(c)} \approx \mathcal{X}$ via Step (3) of the algorithm in Table I	after convergence
I-MD-PWT IV	estimated from $\hat{\mathcal{N}}^{(c)} \approx \mathcal{X}$ via Step (3) of the algorithm in Table I	each iteration

#### IV. NUMERICAL EXAMPLES

We present simulation results comparing the performance of the four variants of the I-MD-PWT approaches in Table II. The parameter settings are set as follows:  $R = 3$ ,  $M_1 = M_2 = M_3 = 7$ ,  $N = 20$ , and  $d = 3$ . The spatial frequencies of the three sources are  $\boldsymbol{\mu}_1 = [\mu_1^{(1)}, \mu_1^{(2)}, \mu_1^{(3)}]^\top = [-0.91, -1.69, -1.19]^\top$ ,  $\boldsymbol{\mu}_2 = [\mu_2^{(1)}, \mu_2^{(2)}, \mu_2^{(3)}]^\top = [-2.22, 1.46, -1.65]^\top$ ,  $\boldsymbol{\mu}_3 = [\mu_3^{(1)}, \mu_3^{(2)}, \mu_3^{(3)}]^\top = [-1.25, -2.75, -1.40]^\top$ . The source samples are i.i.d. ZMCSCG distributed. The Kronecker colored noise is generated according to (3), where along the  $r$ -th mode the colored noise is modeled as a first-order autoregressive (AR) process. The entries of  $\mathbf{L}_r$ ,  $r = 1, \dots, R+1$ , are hence functions of only the AR correlation coefficient  $\rho_r$  [5]. The AR correlation coefficients in the first 3 modes are set as  $\rho_1 = 0.9$ ,  $\rho_2 = 0.5$ , and  $\rho_3 = 0.75$ . The root mean square error (RMSE) defined as

$$\text{RMSE} = \sqrt{\frac{\sum_{r=1}^R \sum_{i=1}^d \left( \hat{\mu}_i^{(r)} - \mu_i^{(r)} \right)^2}{R \times d}}, \quad (11)$$

is used to measure the performance of the proposed prewhitening algorithms. Each result represents an average of 100 independent Monte Carlo runs. The UTE is used for HR. For CFP-PE, similar results are obtained. Therefore, they are not included here to save space. The UTE without prewhitening (UTE w/o PWT) and the UTE with prewhitening (MD-PWT UTE) assuming the knowledge of the noise components are also incorporated as the benchmarks. Their RMSE curves are referred to as the performance lower and upper bounds, respectively.

Figs. 1(a)-(c) show the RMSE trajectories of four I-MD-PWT schemes versus iteration index  $k$ , for three different SNRs: -10 dB, 10 dB, and 20 dB.

For low SNR of -10 dB shown in Fig. 1(a), as  $k$  increases, the RMSEs of all four I-MD-PWT schemes drop and finally reach a stable state. The I-MD-PWT I and I-MD-PWT III converge to a stable state with much lower RMSEs than the I-MD-PWT II and I-MD-PWT IV. One explanation is that for low SNRs, parameter estimates may contain large errors (outliers) depending on the noise realization, which, when HR is incorporated in the iterative process, as that done in I-MD-PWT II and I-MD-PWT IV, are propagated to the reconstructed signals and accumulated and magnified as the iteration proceeds. Such error propagation and magnification occur even for an intermediate SNR of 10 dB (See Fig. 1(b)), particularly in the presence of closely-spaced sources where inaccurate frequency estimates (at least part of them) are obtained. On the contrary, I-MD-PWT I and I-MD-PWT III are free from such error accumulation and magnification, since HR is not applied until convergence.

Note that the I-MD-PWT III and I-MD-PWT IV converge faster and/or converge to a better state (with smaller estimation error) than the I-MD-PWT I and I-MD-PWT II. This is because, for such low SNRs, the noisy measurements are dominated by noise components, and hence the initial settings for the prewhitening matrices  $\hat{\mathbf{L}}_{0,r}$ ,  $r = 1, \dots, R+1$ , in the former two variants are more accurate than those of the latter two. Note also that although with inaccurate initialization of the prewhitening matrices, the I-MD-PWT I converges to the same performance to that of the I-MD-PWT III with only 2 more iterations.

When the SNR is close to 0 dB, none of the four variants performs satisfactorily in the sense that almost no improvement in estimation accuracy is observed compared to that without prewhitening (To save the space, the result is not shown). This may be because, the signal power is comparable to the noise power, in which case neither initialization scheme for  $\hat{\mathbf{L}}_{0,r}$  is accurate. To develop an adaptive I-MD-PWT algorithm whose initial values of the prewhitening matrices vary with the noise level deserves further research and is left as future work.

In Fig. 1(b), we see that outliers resulting from error propagation and magnification occur even for SNR=10 dB. Consequently, the I-MD-PWT II reaches a steady state with large mean estimation error that is close to the upper bound. In contrast, the I-MD-PWT I returns frequency estimates that do not contain outliers and hence has a small RMSE that attains the lower bound.

For a high SNR of 20 dB, as shown in Fig. 1(c), both I-MD-PWT I and II achieve the same best performance with

only a few iterations, although the latter takes 1 more iteration to converge. Moreover, for higher SNRs, the same number of iterations is required for them to converge to the performance upper bound.

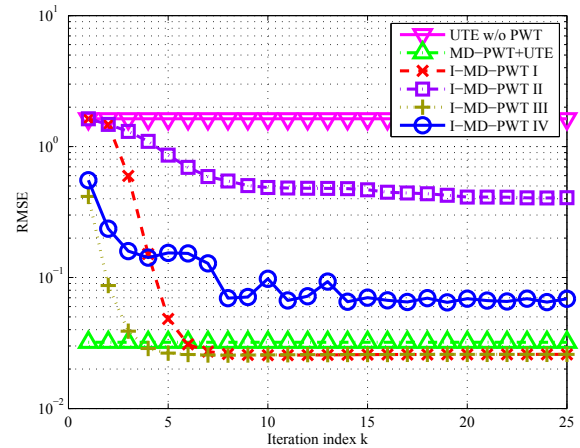
Note that for intermediate and high SNRs, the I-MD-PWT III and IV fail to work or perform badly due to inaccurate initialization of the prewhitening matrices.

## V. CONCLUSION

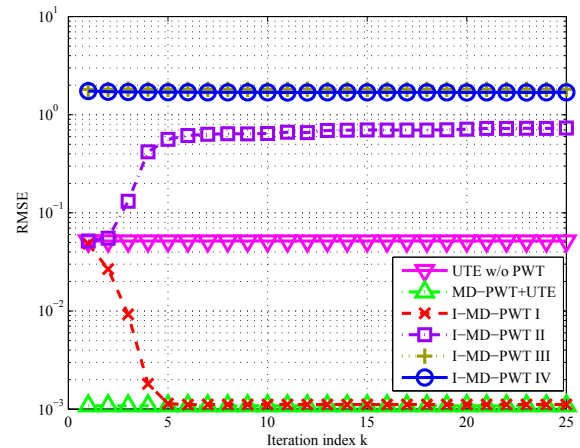
In case noise-only observation samples are unavailable, recently an iterative algorithm for joint prewhitening and harmonic retrieval has been proposed for a good separation of signal and noise subspaces, leading to efficient noise reduction and enhanced HR. We investigate the effect of 1) the initialization of the prewhitening matrices and 2) whether the parametric signal structure is exploited or not during the iterations, on the prewhitening performance of the iterative algorithm. Extensive simulations show that, neglecting the parametric signal structure in the iterations leads to more stable performance with higher probability of convergence, particularly under low-to-intermediate SNR conditions. On the other hand, the iterative prewhitening algorithm is not sensitive to the initialization of the prewhitening matrices.

## REFERENCES

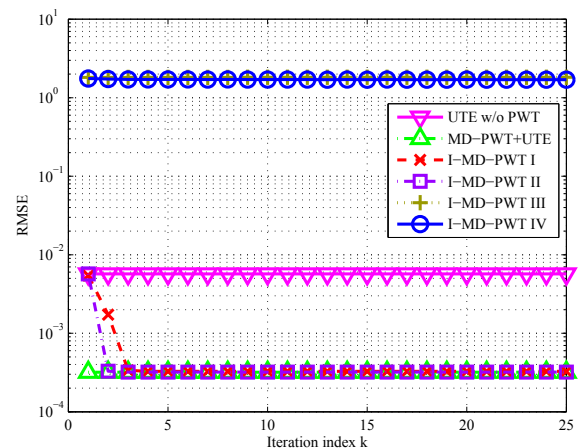
- [1] M. Haardt, J. A. Nossék, Simultaneous Schur decomposition of several non-symmetric matrices to achieve automatic pairing in multidimensional harmonic retrieval problems, *IEEE Transactions on Signal Processing* 46, No. 1 (1998) 161–169.
- [2] M. Haardt, F. Roemer, G. DeL Galdo, Higher-order SVD based subspace estimation to improve the parameter estimation accuracy in multidimensional harmonic retrieval problems, *IEEE Transactions on Signal Processing* 56 (7) (2008) 3198–3213.
- [3] H. L. van Trees, *Optimum Array Processing: Detection, Estimation, and Modulation Theory*, New York: Wiley, 2002, Part IV.
- [4] W. Sun, H. C. So, F. K. W. Chan, L. Huang, Tensor approach for eigenvector-based multi-dimensional harmonic retrieval, *IEEE Transactions on Signal Processing* 61 (13) (2013) 3378–3388.
- [5] J. P. C. L. da Costa, K. Liu, H. C. So, S. Schwarz, M. Haardt, F. Römer, Multidimensional prewhitening for enhanced signal reconstruction and parameter estimation in colored noise with Kronecker correlation structure, *Signal Processing* 93 (11) (2013) 3209–3226.
- [6] L. De Lathauwer, B. De Moor, J. Vandewalle, A multilinear singular value decomposition, *SIAM J. Matrix Anal. Appl.* 21 (4) (2000) 1253–1278.
- [7] M. Pesavento, Fast algorithm for multidimensional harmonic retrieval, Ph.D. thesis, Electrical Engineering and Information Sciences, Ruhr-Universität Bochum, Bochum, Germany (Feb. 2005).
- [8] N. D. Sidiropoulos, R. Bro, G. B. Giannakis, Parallel factor analysis in sensor array processing, *IEEE Transactions on Signal Processing* 48 (8) (2000) 2377–2388.
- [9] B. Park, T. F. Wong, Training sequence optimization in MIMO systems with colored noise, in: *Military Communications Conference (MILCOM 2003)*, Gainesville, USA, 2003, pp. 135–140.
- [10] L. Beltrachini, N. von Ellenrieder, C. Muravchik, Shrinkage approach for spatiotemporal EEG covariance matrix estimation, *IEEE Transactions on Signal Processing* 61 (7) (2013) 1797–1808.
- [11] F. Römer, M. Haardt, A closed-form solution for multilinear PARAFAC decompositions, in: *Proc. 5th IEEE Sensor Array and Multichannel Signal Processing Workshop (SAM'08)*, Darmstadt, Germany, 2008, pp. 487–491.



(a) SNR= -10 dB



(b) SNR=10 dB



(c) SNR=20 dB

Figure 1. RMSE of the frequency estimates versus number of iterations under different SNR conditions.